

Infrared Radiation from Hot Jupiters

Drake Deming¹, L. Jeremy Richardson², Sara Seager³, Joseph Harrington⁴

¹*Planetary Systems Laboratory, NASA's Goddard Space Flight Center, Code 693, Greenbelt, MD 20771 USA
[ddeming@pop600.gsfc.nasa.gov]*

²*NRC Research Associate in the Exoplanet and Stellar Astrophysics Laboratory, NASA's Goddard Space Flight Center, Code 667, Greenbelt MD 20771 USA
[richardsonlj@milkyway.gsfc.nasa.gov]*

³*Department of Terrestrial Magnetism, Carnegie Institution of Washington, 5241 Broad Branch Road NW, Washington, DC 20015 USA [seager@dtm.ciw.edu]*

⁴*Center for Radiophysics and Space Research, Cornell University, 326 Space Sciences Bldg., Ithaca, NY 14853-6801 USA
[jh@oobleck.astro.cornell.edu]*

Abstract. Recent Spitzer infrared (IR) observations of two transiting hot Jupiters during their secondary eclipses have provided the first direct detection of planets orbiting other stars (Charbonneau et al. 2005; Deming et al. 2005). We here elaborate on some aspects of our detection of HD 209458b at 24 μm , and we compare to the detection of TrES-1 by Charbonneau et al. Spitzer will eventually determine the IR spectral energy distribution of these and similar hot Jupiters, opening the new field of comparative exoplanetology. For now, we have only three Spitzer data points, augmented by upper limits from the ground. We here interpret the available measurements from a purely observational perspective, and we point out that a blackbody spectrum having $T \sim 1100\text{K}$ can account for all current IR measurements, within the errors. This will surely not remain true for long, since ongoing Spitzer observations will be very sensitive to the IR characteristics of hot Jupiters.

1. Direct Detection of Extrasolar Planets

There are now over 160 extrasolar planets known from Doppler surveys, and about 15% of these are hot Jupiters. Strong stellar irradiation heats these planets to $T > 1000\text{K}$ (Seager and Sasselov 1998), so they should emit most of their radiation in the IR. A number of pioneering attempts were made to detect hot Jupiters from the ground in the combined IR light of star+planet (Wiedemann et al. 2001, Lucas and Roche 2002, Richardson et al. 2003a,b). But success was only recently achieved, and it required using the Spitzer Space Telescope (Charbonneau et al. 2005; Deming et al. 2005).

The Spitzer observations of two hot Jupiters are the first direct detections of extrasolar planets. To be clear about terminology, by direct detection we mean that photons emitted by the planet are detected, and are separated from stellar photons by some method. One method to separate the stellar and planetary photons would be to spatially resolve the planet and the star, e.g., by imaging. Imaging of extrasolar planets is being widely pursued, but it requires a very high order of technology. The technique which is successful for Spitzer is to observe the *secondary eclipse* of transiting hot Jupiters. We measure the star+planet when the planet is out of eclipse, and the star alone when the planet is eclipsed, and the difference tells us how many photons are due to the planet.

Note that the secondary eclipse technique does not specify *which* of the detected photons are due to the planet, and which are from the star, only *how many* photons are from the planet. But for scientific purposes, ‘how many’ is the primary quantity of interest! So secondary eclipses are a very sensitive and useful method for direct detection and characterization of transiting extrasolar planets. There are *nine* ongoing Spitzer programs to detect and characterize close-in extrasolar planets in combined IR light, and we are now truly in the era of comparative exoplanetology.

In Sec 2, we describe our detection of the secondary eclipse of HD 209458b, elaborating on some points not mentioned in our detection paper. Sec. 3 interprets our results in combination with the TrES-1 measurements by Charbonneau et al. (2005), and factors in the ground-based upper limits. We point out the importance of measuring these planets in the 2- to 5- μm wavelength region, where there is currently a considerable question about their level of IR emission.

2. The Secondary Eclipse of HD 209458b

Figure 1 shows the secondary eclipse of HD 209458b at 24 μm wavelength, observed using the Multiband Imaging Photometer for Spitzer

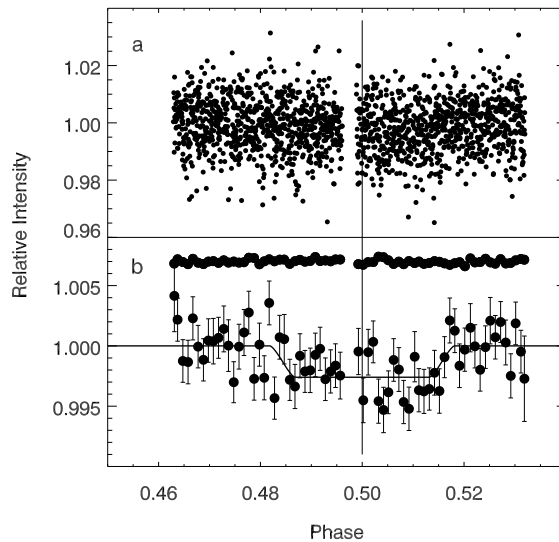


Figure 1.: *Photometric detection of the secondary eclipse of HD 209458b using Spitzer/MIPS. The upper panel shows all 1696 individual photometric points, which are binned in the lower panel to show the eclipse. The fitted eclipse curve is overplotted. The points above the eclipse are a control sequence, showing the stability of the technique. Note that the eclipse is accurately centered at phase 0.5, as marked by the vertical line.*

(MIPS, Rieke et al. 2004). The scatter in the individual points (upper panel) is about 0.008 magnitudes, poorer than is possible from the ground in the visible. However, the MIPS precision is limited by statistical fluctuations in the thermal emission from dust in our own solar system, the IR zodiacal light. The Spitzer data analysis pipeline provides an ‘error image’ which quantifies these statistical fluctuations. We extract the brightness of the star using an optimal weighting technique (Horne 1986), and we propagate the error image thru the same procedure to derive the formal errors in the photometry. We find the scatter in our photometry to be in close agreement with the formal errors. We are background-limited by the thermal zodiacal emission.

In addition to noise from the zodiacal background, there are some instrument quirks in MIPS. For example, there is a ‘first frame’ effect, where the signal from the MIPS detector is different if it has just been reset. Fortunately, we were able to use a simple trick to remove the instrument quirks. Our trick is to ratio the intensity of the star to the

total intensity of the zodiacal background in the image. Since the background is a large signal, its relative precision is much better than the star's precision, and the ratio does not add significant additional noise. Moreover, because of Spitzer's modest (0.85-meter) aperture, diffraction spreads the stellar image over multiple pixels, like the background. Also, the per-pixel intensity of the star is only modestly greater than the background. To MIPS, the star looks like a small patch of bright background, so the instrument treats the background and stellar photons exactly the same - it cannot 'tell the difference'. After normalizing the stellar intensity to the background, we find the instrument quirks are gone, and the noise is accurately characterized as Gaussian white noise, which averages down as the square-root of the number of observations - just as the text books predict.

The lower panel of Figure 1 averages our secondary eclipse photometry into bins of 0.001 in phase, and adds error bars to the binned values. Now the secondary eclipse is quite evident, and is seen to be centered at phase 0.5. We fit an eclipse curve to the data, and find a best-fit depth of $0.26 \pm 0.046\%$, a 5.6σ detection. The planet's brightness temperature is $1130 \pm 150\text{K}$. Simultaneously with our MIPS detection of HD 209458b, Charbonneau et al. (2005) detected TrES-1 at 8- and $4.5\text{-}\mu\text{m}$ using Spitzer's InfraRed Array Camera (IRAC). The TrES-1 measurements imply a very similar temperature (1060K), and their $8\text{ }\mu\text{m}$ measurement has over 6σ statistical significance. Since these three data points are (so far) our only direct measurements of hot Jupiters, they have elicited considerable interest. Four modeling papers have interpreted the measurements (Barman et al. 2005, Burrows et al. 2005, Fortney et al. 2005, Seager et al. 2005), but in Sec. 3 we will give a more simple-minded interpretation, highlighting what we call the 'short IR wavelength question'.

The Spitzer detections have been described as surprising, in the sense of being unexpected. Certainly this application for Spitzer was unanticipated in the early years when the observatory was being developed. But recently, the planet-to-star contrast ratio was robustly predicted to be a significant fraction of one percent at long IR wavelengths (Charbonneau 2003, Burrows et al. 2004). Prior to launch, we reasoned that if we couldn't detect a fraction of one percent using a cryogenic telescope in space, then we should surely give up! Fortunately, the first public data from MIPS showed us that Spitzer's sensitivity and stability were up to the task. So we knew in advance that we would detect HD 209458b with MIPS, providing that the planet was at least as hot as 700K - which seemed unavoidable.

Curiously, the Spitzer detections did not start with the best cases. Since the flux from both the planet and star decrease with wavelength (decline of the Planck function), $24\text{ }\mu\text{m}$ is not the best wavelength for

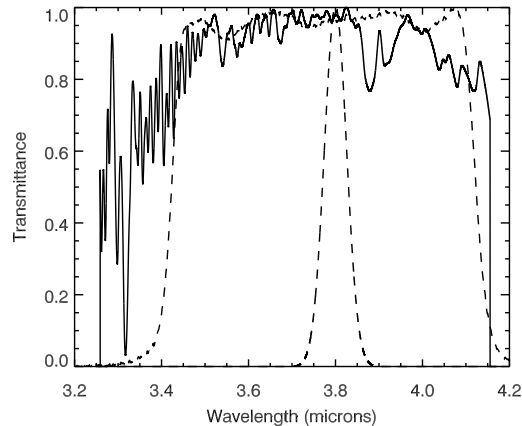


Figure 2.: *Window in the terrestrial atmosphere for photometry of hot Jupiters at 3.8 μm . The solid line shows the telluric transmittance at moderate spectral resolution. The dashed curves are the transmittance of the conventional L' filter (broad), and our CVF (narrow).*

secondary eclipse detection. The IRAC 8 μm channel is more suitable, being source photon-limited, not background-limited. But for historical reasons, IRAC was first used by Charbonneau et al. for TrES-1, not for HD 209458. So the brighter and closer system was not observed at the best wavelength. The new observing programs now underway will soon fill this gap, and we will see secondary eclipses of hot Jupiters even more clearly. The new very hot Jupiter recently announced by Bouchy et al. (2005) will be an especially important target for Spitzer.

3. The Short IR Wavelength Question

3.1 New 3.8 μm Photometry

In order to discuss what we regard as the major unresolved observational question concerning hot Jupiters, we need to include the ground-based data. A flux peak is predicted to occur in hot Jupiter spectra at 3.8 μm (Sudarsky et al. 2003). Ground-based observations can be very useful at this important wavelength, because we can use a filter centered exactly on the predicted peak (the IRAC bandpasses are offset). Unfortunately, the high thermal background from the ground has made broadband photometry impossible near 4 μm - most instrument detector arrays saturate in quite short integration times.

In September 2003 we obtained 3.8 μm photometry of HD 209458 during two secondary eclipses, using NSFCAM (Shure et al. 1994) on the NASA Infrared Telescope Facility (IRTF). We were able to avoid detector saturation by using a narrow optical bandwidth, a 1.5% circular-variable-filter (CVF). Figure 2 shows the atmospheric transmittance, and the profile of the conventional L' filter, and our CVF at 3.8 μm . To monitor changes in atmospheric absorption, we observed a comparison star of similar brightness to HD 209458. We have completed the analysis of one of the two eclipses. The eclipse amplitude in that case, from 329 individual 10-second exposures, was -0.0007 ± 0.0014 , i.e. the system nominally becomes brighter when the planet is hidden, consistent with seeing no eclipse. Not surprisingly, the errors are larger in the ground-based observations than with Spitzer, but nevertheless the results are sufficiently precise to be somewhat puzzling, as we explain below.

3.2 An Observational Perspective

The two extrasolar planets currently observed by Spitzer - HD 209458b and TrES-1 - are different worlds, and they surely have their own unique characteristics. But, our ignorance of hot Jupiter spectra is arguably much greater than the real differences between them. So here we compare observations of both planets to a single model. To quantify the similarity between the two planets, we assume thermal equilibrium and the same Bond albedos and efficiency of heat redistribution. In the long wavelength (Rayleigh-Jeans) limit, it is easy to show that the planet-to-star contrast c_λ depends on the stellar and orbital parameters as:

$$c_\lambda \sim R_p^2 R_*^{-\frac{3}{2}} a^{-\frac{1}{2}} \quad (1)$$

where R_p and R_* are the planetary and stellar radius, respectively, a is the orbit semi-major axis, and we suppress the constant containing the Bond albedo. Note that the temperature of the star does not appear since it cancels when computing the contrast. Using the parameters for HD 209458 (Brown et al. 2001; Wittenmyer 2005) and TrES-1 (Alonso et al. 2004), we find that the contrasts for these two systems at a given wavelength would differ by only 8% under our simple assumptions. So comparing them to a single model is reasonable.

Figure 3 shows contrast versus wavelength for HD 209458b and TrES-1, and compares the observations to a model from Sudarsky et al. (2003), as did Charbonneau et al. (2005, their Figure 3). The dashed line is the contrast from a blackbody having $T = 1100\text{K}$. The Spitzer observations cannot in themselves discriminate between the model curve and a simple blackbody. Considering the errors, all three Spitzer ob-

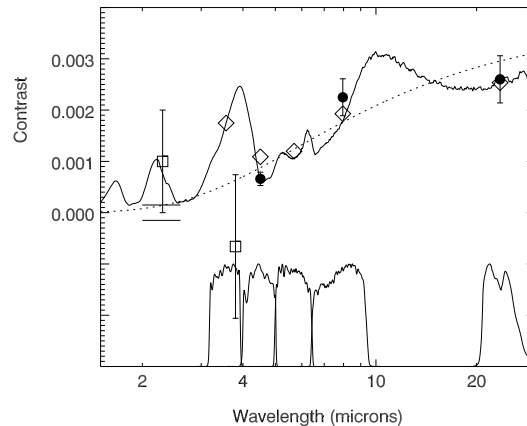


Figure 3.: *Spitzer* and ground-based observations of *TrES-1* and *HD 209458b* in contrast units, compared to a single model (solid line) and 1100K blackbody (dotted line). The *Spitzer* IRAC and MIPS bandpass functions are plotted below. Filled symbols are the *Spitzer* points, and the open diamonds show the expectation value of the contrast averaged over the *Spitzer* bands. The open squares show the ground-based photometry of Snellen (2005) at 2.3 μm , and from this paper at 3.8 μm . The two horizontal lines at 2.2 μm represent the limit from Richardson et al. (2003b). Note log scale for wavelength.

servations could be consistent with either the Sudarsky et al. model or the blackbody.

Now we consider the ground-based data. The error bar on our CVF photometry at 3.8 μm misses the Sudarsky et al. peak at this wavelength, but it overlaps the blackbody. The Snellen (2005) photometry at 2.3 μm agrees with the model, but the error bar also includes the blackbody curve. The most stringent ground-based point is the Richardson et al. (2003b) upper limit at 2.2 μm . This is a limit, derived from differential spectroscopy, on the shape of the spectrum, and it is given by the two horizontal lines. Unlike the other error limits on the figure, this is a 3σ , not 1σ limit. These lines are relative limits, i.e. only the intensity interval between them is significant (see Seager et al. 2005). To conform to this limit, the contrast spectrum has to fit within the lines. The Sudarsky et al. model doesn't fit, but the blackbody does. This is the essence of the short-IR wavelength question - we don't see the peaks predicted in the spectrum where planet flux should escape between absorption bands, and we wonder how strong these peaks re-

ally are. Now, we do not seriously suggest that the planet is actually a blackbody. But to date, we do not have a definitive measurement of departures from a blackbody spectrum in the IR. The IRAC band at $3.5 \mu\text{m}$ should provide this, as evident from Figure 3. Observations of TrES-1 at $3.5 \mu\text{m}$ were made by Spitzer in September 2005, and are now being analyzed by Dave Charbonneau. We eagerly await the results.

References

- Alonso, R., & 11 co-authors 2004, ApJ 613, L153.
- Barman, T. S., Hauschildt P. H., & Allard, F. 2005, ApJ 632, 1132.
- Bouchy, F., & 11 co-authors 2005, Astr. Ap., in press.
- Brown, T. M., Charbonneau, D., Gilliland, R. L., Noyes, R. W., & Burrows, A. 2001, ApJ 552, 699.
- Burrows, A., Hubeny, I., & Sudarsky, D. 2005, ApJ 625, L135.
- Burrows, A., Sudarsky, D. & Hubeny, I. 2004, in *The Search for Other Worlds*, AIP Conf. Proceedings, 713, 143.
- Charbonneau, D. 2003, in *Scientific Frontiers in Research on Extrasolar Planets*, ASP Conf. Series, 294, 449.
- Charbonneau, D., & 10 co-authors 2005, ApJ 626, 523.
- Deming, D., Seager, S., Richardson, L. J., & Harrington, J. 2005, Nature 434, 740.
- Fortney, J. J., Marley, M. S., Lodders, K., Saumon, D., & Freedman, R. 2005, ApJ 627, L69.
- Horne, K. 1986, PASP 98, 609.
- Lucas, P. W. & Roche, P. E. 2002, MNRAS 336, 637.
- Richardson, L. J., and 6 co-authors 2003a, ApJ, 154, 583.
- Richardson, L. J., Deming, D., & Seager, S. 2003b, ApJ 597, 581.
- Rieke, G. H. & 42 co-authors 2004, ApJ(Suppl) 154, 25.
- Seager, S. & Sasselov, D. D. 1998, 502, L157.
- Seager, S., Richardson, L. J., Hansen, B. M. S., Menou, K., Cho, J. Y.-K., & Deming, D. 2005, ApJ 632, 1122.
- Shure, M. A., Toomey, D. W., Rayner, J. T., Onaka, P. M., & Denault, A.J. 1994, SPIE 2198, 614.
- Snellen, I. A. G. 2005, MNRAS 363, 211.
- Sudarsky, D., Burrows, A., & Hubeny, I. 2003, ApJ 588, 1121.
- Wiedemann, G., Deming, D., & Bjoraker, G. 2001, ApJ 546, 1068.
- Wittenmyer, R. A., & 12 co-authors 2005, ApJ 632, 1157.